Tozasertib attenuates neuronal apoptosis via DLK/JIP3/MA2K7/JNK pathway in early brain injury after SAH in rats

Cheng Yin[a,b], **Guang-fu Huang**[b], **Xiao-chuan Sun**[c], **Zongduo Guo**[c], and **John H. Zhang**[a]

[a]Departments of Anesthesiology and Physiology, Loma Linda University School of Medicine, Loma Linda, California

[b]Department of Neurosurgery, Hospital of the University of Electronic Science and Technology of China, Sichuan Provincial People's Hospital, Chengdu, China

[c]Department of Neurosurgery, First Affiliated Hospital of Chongqing Medical University, Chongqing, China

Abstract

Background and Purpose—Since tozasertib is neuroprotective for injured optic nerve, this study is intended to test whether tozasertib reduces early brain injury after subarachnoid hemorrhage (SAH) in a rat model.

Methods—One hundred fifty-five (155) male Sprague-Dawley rats were randomly subjected to endovascular perforation model of SAH and sham group. SAH grade, neurological score, and brain water content were measured at 24 and 72 hours after SAH. Dual leucine zipper kinase (DLK) and its downstream factors, JNK-interacting protein 3 (JIP3), MA2K7, p-JNK/JNK (c-Jun N-terminal kinase), and apoptosis related proteins cleaved caspase-3 (CC-3), Bim, Bcl-2, and cleaved caspase-9 (CC-9) were analyzed by western blot at 24 hours after SAH. Apoptotic cells were detected by terminal deoxynucleotid transferase-deoxyuridine triphosphate (dUTP) nick end labeling (TUNEL). DLK small interfering RNA (siRNA), JIP3 siRNA and MA2K7 siRNA, the JNK, p38MAPK, and MEK inhibitors SP600125, SB203580, and PD98059 were used for intervention.

Results—Tozasertib reduced neuronal apoptosis, attenuated brain edema and improved neurobehavioral deficits 24 and 72 hours after SAH. At 24 hours After SAH, DLK/JIP3/MA2K7/p-JNK/CC-3 expressions were elevated markedly and tozasertib reduced DLK, MA2K7/p-JNK/CC-3 expressions but enhanced JIP3 expression. In the presence of tozasertib, DLK/JIP3/MA2K7 siRNA and SP600125, SB203580 and PD98059 deteriorated the neurobehavioral deficits, brain edema and increased the expression of CC-3. SAH potentiated the

[#]Correspondence to John H. Zhang, MD, PhD, Department of Physiology and Pharmacology, Loma Linda University, School of Medicine, 11041 Campus St, Risley Hall, Room 219, Loma Linda, CA 92354, USA, johnzhang3910@.yahoo.com.

Disclosure: none

expression of Bim, CC-9, and CC-3 but reduced Bcl-2, while tozasertib reduced expression of Bim, CC-9, and CC-3 but enhanced Bcl-2.

Conclusions—Tozasertib reduced neuronal apoptosis and improved outcome possibly via DLK/JIP3/MA2K7/JNK pathways after SAH.

Keywords

subarachnoid hemorrhage; early brain injury; tozasertib; DLK; apoptosis

1. Introduction

Subarachnoid hemorrhage (SAH) is a deadly stroke subtype with high mortality and morbidity (Etminan, 2015; Grunwald et al., 2014). Cerebral vasospasm, hydrocephalus and early brain injury are regarded as the major complications after SAH (Chen et al., 2013a; Hasegawa et al., 2015). Early brain injury starts from the onset of SAH and lasts up to 72 hours (Kusaka et al., 2004; Suwatcharangkoon et al., 2015). One of the major pathological changes of early brain injury is neuronal apoptosis (Caner et al., 2012). Therefore, prevention and reduction of apoptosis may be a target for intervention and treatment for early brain injury.

Tozasertib is a molecular-targeted compound and it has been used in the treatment of chronic myelogenous leukemia and different tumors in clinical trials (Harrington et al., 2004; Huang et al., 2008). Tozasertib improved the survival of injured retinal ganglion cells (RGCs) possibly by inhibition of dual leucine zipper kinase (DLK/MA3K12) (Ferraris et al., 2013). DLK belongs to mitogen-activated protein kinase kinase kinase (MA3K) family. There are studies demonstrated that DLK has participated in apoptosis and neuronal degeneration as well as neural development (Chen et al., 2008; Ghosh et al., 2011).

However, the potential effect of tozasertib for early brain injury after SAH has not been investigated. In this study, we examined the effect and mechanisms of tozasertib on neurological outcomes after SAH in a rat model.

2. Materials and Methods

2.1. Experimental Animals

All experimental procedures were designed and conducted in accordance with the National Institutes of Health Guide for the care and use of laboratory animals and were approved by the Institutional Animal Care and Use Committee (IACUC) of Loma Linda University. Two hundred sixteen (216) male Sprague-Dawley rats (280–350g in weight; Harlan, Indianapolis, IN) were used in sham and SAH groups. All rats were resided in a light and temperature-controlled room with sufficient food and water.

2.2. SAH Model and Study Design

SAH model was executed by endovascular perforation for the induction of SAH as previously described (Song et al., 2015; Zhan et al., 2015). Briefly, rats were deeply anesthetized by isoflurane. Anesthesia was maintained with 3% isoflurane in 70%/30%

medical air/oxygen. A 4-0 nylon suture with a sharp tip was plugged in the left internal carotid artery and propelled until resistance was felt at the bifurcation of the anterior and middle cerebral artery. Then, inserting the suture an extra 3mm to puncture the middle cerebral artery. The suture was promptly retracted to allow blood reperfusion in internal carotid artery, leaded to SAH. Sham rats received the same procedures without the vessel perforation.

All rats were randomly assigned to the following studies:

(1) Outcome study: Sham group (n=14), SAH group (n=12), SAH+vehicle group (n=15), SAH+tozasertib (1μg) group (n=18), SAH+tozasertib (5μg) group (n=15); (2) Mechanism study: Sham group (n=6), SAH+vehicle group (n=7), SAH +tozasertib group (n=7), SAH+tozasertib+vehicle group (n=12), SAH+tozasertib +scramble siRNA group (n=13), SAH+tozasertib+DLK siRNA group (n=15), SAH +tozasertib+JIP3 siRNA group (n=13), SAH+tozasertib+MA2K7 siRNA group (n=14), SAH+tozasertib+vehicle group (n=13), SAH+tozasertib+SP600125 group (n=14), SAH+tozasertib+SB203580 group (n=15), SAH+tozasertib+PD98059 group (n=13).

2.3. SAH Grade

After euthanasia and removing the rat's brain, the base of the brain was photographed immediately and divided into six predetermined areas as previously described (Sugawara et al., 2008). Basing on the amount of blood, each area was given a score from 0 to 3. All area scores were added as the total SAH grade (maximum SAH grade=18). Fifteen rats with mild SAH whose SAH grades 7 were excluded from the study.

2.4. Neurological Score

At 24 hours after SAH, neurological function was evaluated with blinded fashion by the modified Garcia score (Garcia et al., 1995) and beam balance test (Chen et al., 2013b). The modified Garcia score included six subtests accessing the animal's spontaneous activity. Each subtest was given a score from 0 to 3, and the total score reflected the neurological function (maximum score =18). For the beam balance test, rats were arranged to walk on a 15 mm-wide wooden beam for 1 minute. The score ranged from 0 to 4 was determined by the walking distance. The average score of three consecutive tests was calculated. Higher scores represented better neurological function.

2.5. Brain Water Content

At 24 hours after SAH, the left hemisphere, right hemisphere, cerebellum, and brain stem were separated swiftly, and each part was immediately weighed (wet weight). After dehydration in 105°C for 72 hours, brain part was weighed again (dry weight). The percentage of water content was calculated as (wet weight–dry weight)/wet weight (Liu et al., 2014).

2.6. Intracerebroventricular Injection Administration

Intracerebroventricular injection administration was executed as previously described (Chen et al., 2015; Tang et al., 2015). Briefly, rats were laid in a stereotaxic apparatus under 2.5% isoflurane anesthesia. The 10 μL needle of Hamilton syringe (Microliter 701; Hamilton Company, Reno, NV) was plugged through a burr hole into the left lateral ventricle. Intracerebroventricular administration was conducted by a microinfusion pump (Harvard Apparatus, Holliston, MA) at a rate of 0.5μL/minute. Followings were the reagents of intracerebroventricular injection administration: (1) SiRNA: sterile phosphate buffered saline (PBS) 5μL served as siRNA and scramble siRNA vehicle control. All siRNA (500 pmol/5μL, Santa Cruz Biotechnology, Santa Cruz, CA) were injected at 24 hours before SAH production.

DLK siRNA:

  a. sense, GCUCAGGCGAGAGCAAGCUUUAGAA, antisense, UUCUAAAGCUUGCUCUCGCCUGAGC;

  b. sense, CCCUCAUGUUGCAACUAGAACUCAA, antisense, UUGAGUUCUAGUUGCAACAUGAGGG;

  c. sense, CCAAUAGUGUCCUGCAGCUACAUGA, antisense, UCAUGUAGCUGCAGGACACUAUUGG;

JIP3 siRNA:

  a. sense, AGCGUCCCACCUCUCUGAAUGUCUU, antisense, AAGACAUUCAGAGAGGUGGGACGCU;

  b. sense, UGGCAGUUCUUUAGCCGCCUCUUCA, antisense, UGAAGAGGCGGCUAAAGAACUGCCA;

  c. sense, CAGCUGGCUUUAGCCAGCGUCGCAA, antisense, UUGCGACGCUGGCUAAAGCCAGCUG;

MA2K7 siRNA:

  a. sense, CCUUGUUCACACCUCGCAGTT, antisense, CUGCGAGGUGUGAACAAGGTT;

  b. sense, GGATCGACCTCAACCTGGATAT, antisense, CCAGCGTTATCAGGCAGAAATC;

  c. sense, CCCTACATTGTTCAGTGCTTTG, antisense, CAGTGCTTTGGTACCTTCATCA.

  (2) Tozasertib (1μg/5μg, BioVision, Milpitas, CA) was dissolved by 5μL PBS (5μL PBS served as the vehicle control). Tozasertib was injected at 2 hours after SAH.

  (3) JNK, p38MAPK, and MEK inhibitors SP600125, SB203580, and PD98059 (10 pmol, Santa Cruz Biotechnology, Santa Cruz, CA) were dissolved by 5μL PBS (Tu et al., 2015; Wei et al., 2015; Yatsushige et al., 2008) (5μL PBS served as the vehicle control). Those inhibitors were injected at 20 min before SAH.

2.7. TUNEL Staining

For double staining of NeuN and terminal deoxynucleotid transferase-deoxyuridine triphosphate (dUTP) nick end labeling (TUNEL), a TUNEL kit (In situ Cell Death Detection Kit, Fluorescein, Roche, Mannheim, Germany) was used after the slices were incubated with anti-NeuN primary antibody and Texas Red-conjugated secondary antibody. For quantitative analyses, TUNEL-positive neurons were counted in the left cortex-facing blood clots (4 different areas in 500×500 μm grids) by a blinded investigator. Data were expressed as cells/mm (Topkoru et al., 2013).

2.8. Western Blot

The cerebral cortex tissues that facing blood clots were collected at 24 hours after SAH. Western blot was performed as described previously (Li et al., 2014). Primary antibodies used in western bolt were DLK (Santa Cruz Biotechnology, Santa Cruz, CA), JIP3 (MyBioSource, San Diego, CA), MA2K7 (MyBioSource, San Diego, CA), p-JNK (Santa Cruz Biotechnology, Santa Cruz, CA), JNK (Santa Cruz Biotechnology, Santa Cruz, CA), cleaved caspase-3 (CC-3, Cell Signaling Technology, Danvers, MA), actin (Santa Cruz Biotechnology, Santa Cruz, CA), Bim (Santa Cruz Biotechnology, Santa Cruz, CA), Bcl-2 (Cell Signaling Technology, Danvers, MA) and cleaved caspase-9 (CC-9, Millipore, Billerica, MA).

2.9. Statistical Analysis

Data are expressed as mean ±SD. Statistical significance was verified with analysis of variance, followed by Tukey test for multiple comparisons. The probability levels $p < 0.05$ were considered statistically significant. The analysis of mortality was done with χ^2 test. Nonparametric analysis of variance was used for categorical variables.

3. Results

3.1. SAH Grade

Mean SAH severity scores were measured at 24 hours in survived SAH rats, and the mean SAH grading was 12.5 ± 2.2. There was no significant difference in the severity scores across groups.

3.2. Mortality Rates

Mortality rates were as follows: Sham, 0% (0 of 20); SAH, 0% (0 of 12); SAH+vehicle, 9% (2 of 22); SAH+tozasertib (1ug), 20% (5 of 25); SAH+tozasertib (5ug), 20% (3 of 15); SAH + tozasertib +vehicle, 0% (0 of 12); SAH+ tozasertib +scramble siRNA, 8% (1 of 13); SAH + tozasertib +DLK siRNA, 7% (1 of 15); SAH+ tozasertib +JIP3 siRNA, 8% (1 of 13); SAH + tozasertib +MA2K7 siRNA, 14% (2 of 14); SAH+ tozasertib +vehicle, 8% (1 of 13); SAH + tozasertib +SP600125, 14% (2 of 14); SAH+ tozasertib +SB203580, 20% (3 of 15); SAH+ tozasertib +PD98059, 8% (1 of 13). No statistical significances were identified among groups ($p > 0.05$).

3.3. Effects of tozasertib on neurobehavioral deficits and brain edema after SAH

Two dosage of tozasertib(1μg/5μg) were injected into the left ventricle at 2 hours after SAH surgery. The neurological scores and brain water content were measured at 24 hours and 72 hours after SAH.

At 24 hours after SAH, tozasertib (1μg) significantly improved the modified Garcia score ($p<0.05$; Fig. 1. A) and the beam balance score ($p<0.05$; Fig. 1. C). Tozasertib (1μg) decreased brain water content in left and right hemispheres of the brain ($p<0.05$; Fig. 1. E). Tozasertib (5μg) only significantly decreased the brain water content in left hemispheres of the brain ($p<0.05$; Fig. 1. E), but did not significantly improved the modified Garcia score and beam balance score ($p>0.05$; Fig. 1. A. C).

At 72 hours after SAH, tozasertib (1μg) significantly improved the modified Garcia score ($p<0.05$; Fig. 1. B), but not the beam balance score ($p>0.05$; Fig. 1. D). Tozasertib (5μg) did significantly improved the modified Garcia score and beam balance score ($p>0.05$; Fig. 1. B. D). Tozasertib (1μg/5μg) decreased the brain water content in left and right hemispheres of the brain ($p<0.05$; Fig. 1. F).

3.4. Effects of tozasertib on neuronal apoptosis after SAH

Since the above mentioned results indicated that the low dosage of tozasertib (1μg) was more effective on neurobehavioral score and brain water content, we decided to use the low dosage for the following studies.

Immunofluorescence staining showed the increased number of TUNEL and NeuN double-stained cells (TUNEL+neurons) in the left cortex after SAH when compared to the sham group ($p<0.05$; Fig. 2). Tozasertib (1μg) reduced the number of TUNEL+neurons cells in the left cortex when compared to the SAH+vehicle group at 24 hours after SAH ($p<0.05$; Fig. 2).

3.5. Effects of tozasertib on DLK, JIP3, MA2K7, p-JNK/JNK, and CC-3 expression at 24 hours after SAH

In SAH+vehicle group, the DLK and its downstream proteins were increased when compared to the sham group ($p<0.05$; Fig. 3. A. B. C. D. E. F). Tozasertib (1μg) reduced the expression of DLK, MA2K7, p-JNK and CC-3 when compared with SAH+vehicle group ($p<0.05$; Fig. 3. A. B. D. E. F), while JIP3 expression was significantly increased compared to SAH+vehicle group ($p<0.05$; Fig. 3. A. C).

3.6. Effect of DLK/JIP3/MA2K7 siRNA on the effect of tozasertib on neurobehavioral deficits, brain edema and CC-3 at 24 hours after SAH

Tozasertib improved the modified Garcia score ($p<0.05$; Fig. 1. A) and the beam balance score ($p<0.05$; Fig. 1. C) at 24 hours after SAH, and the above mentioned effects of tozasertib were reduced by DLK siRNA ($p<0.05$, Fig. 4. A, B). The alleviating effect of tozasertib on brain edema was also reduced by DLK siRNA in left and right hemispheres of the brain. JIP3 siRNA only decreased the above mentioned effect in left hemispheres of the brain ($p<0.05$, Fig. 4. C). Tozasertib reduced the level of CC-3 and the effects of tozasertib

were countered by DLK/JIP3, and slightly by MA2K7 siRNA in the left cortex after SAH (p<0.05; Fig. 4. D). DLK/JIP3/MA2K7 siRNA was administered 24 hours before SAH and tozasertib (1μg) was used 2 hours after SAH.

3.7. Effect of JNK/p38MAPK/MEK inhibitors on the effect of tozasertib on neurobehavioral deficits, brain edema and CC-3 at 24 hours after SAH

In addition to the above-described siRNAs, the JNK, p38MAPK and MEK inhibitors SP600125, SB203580, and PD98059 were administered at 20 min before SAH, and tozasertib was administered at 2 hours after SAH. The improved effects of tozasertib on modified Garcia and beam balance score were significantly inhibited by JNK/p38MAPK inhibitors without MEK inhibitors (p<0.05, Fig. 5. A, B). The alleviating effect of tozasertib on brain edema in left and right hemispheres of the brain were significantly inhibited by JNK/p38MAPK inhibitors without MEK inhibitors (p<0.05, Fig. 5. C). Tozasertib reduced the level of CC-3 and the effects of tozasertib were significantly countered by JNK and p38MAPK inhibitors SP600125, SB203580, and slightly by and MEK inhibitor PD98059 in the left cortex (p<0.05; Fig. 5. D).

3.8 Effect of tozasertib on other apoptosis factors at 24 hours after SAH

In SAH+vehicle group, the levels of Bim, CC-9 and CC-3 were increased and Bcl-2 decreased when compared to sham group (p<0.05; Fig. 6). Tozasertib (1μg) reduced the levels of Bim, CC-9 and CC-3 and increased Bcl-2 (p<0.05; Fig. 6).

4. Discussion

Tozasertib, also called VX-680 or MK-0457, is an inhibitor of aurora kinases and some other kinases (Tyler et al., 2007). Tozasertib has been tentatively used to treat cancer/tumor patients by facilitating apoptotic activity (Harrington et al., 2004; Michaelis et al., 2014). Welsbie et al. reported that tozasertib may be neuroprotective in rat optic nerve transection. Low dosage of tozasertib (1μM/L) improved cultured RGCs survival (Welsbie et al., 2013). In this study, we observed that tozasertib reduced TUNEL positive neurons, decreased brain edema and improved neurobehavioral function after SAH. The effects of tozasertib seemed mediated by DLK/JIP3/MA2K7/JNK pathways. DLK/JIP3/MA2K7 siRNA and JNK, p38MAPK and MEK inhibitors SP600125, SB203580, and PD98059 all countered the effect of tozasertib on the neurobehavioral deficits, brain edema and levels of CC-3. In addition, tozasertib reduced the levels of Bim, CC-9 and enhanced Bcl-2.

Although DLK protein distributed extensively in the rat brain, it was detected predominantly in neurons in the adult rat cortex (Mata et al., 1996; Merritt et al., 1999). Several studies demonstrated that DLK regulated multiple pathophysiological processes, related to neural development, axon degeneration and apoptosis (Bloom et al., 2007; Ghosh et al., 2011; Hirai et al., 2011; Hirai et al., 2006; Hirai et al., 2002; Itoh et al., 2011). DLK combined with JIP3 to form a signaling complex which activates MA2K7 and p-JNK (Ghosh et al., 2011; Merritt et al., 1999). The expression of DLK was increased after optic nerve transaction and down-regulation of DLK improved the survival and function of RGCs in vitro and in vivo in rats (Watkins et al., 2013; Welsbie et al., 2013). However, DLK and its downstream factors seem

detrimental in early brain injury after SAH since DLK/JIP3/MA2K7/JNK expression were all increased and tozasertib reduced the expression of DLK, MA2K7, and p-JNK. Tozasertib also reduced Bim, CC-9, CC-3 expressions and TUNEL positive neurons in cerebral cortex after SAH.

Since p-JNK expression was increased after SAH and reduced by tozasertib, we tested the role of JNK, p38MAPK and MEK in apoptotic cell death (Bai et al., 2015; Chang et al., 2003; Feng et al., 2015). In the presence of tozasertib after SAH, inhibition of JNK and p38MAPK deteriorated neurobehavioral deficits, brain edema and enhanced CC-3 levels substantially. MEK inhibitor also slightly deteriorated neurobehavioral deficits and brain edema, but significantly elevated the level of CC-3. Those observations indicate that tozasertib reduced apoptosis may be mediated by JNK, p38 and MEK pathways.

In general, apoptosis is consisted by two phases, initiation and execution. The intrinsic (mitochondrial) and extrinsic (death receptors) pathways represented the canonical routes of caspase activation during the initiation phase (Krantic et al., 2007). As a marker protein of cellular apoptosis, CC-3 can be activated by the intrinsic or extrinsic pathway. Since neuronal apoptosis has been reported after SAH (Cahill et al., 2006), our observations of TUNEL positive cells and CC-3 elevation are consistent with published literature. Considering SAH is an acute onset of bleeding stress disorder, it is speculated that the intrinsic pathway may contribute to neuronal apoptosis. Therefore, the expressions of Bim, Bcl-2 and CC-9 which represented intrinsic pathway of apoptosis were examined in this study. We have observed that SAH potentiated the levels of Bim and CC-9 and reduced Bcl-2, and tozasertib reduced Bim and CC-9 but enhanced Bcl-2 and reduced TUNEL positive cells. However, this study does not rule out the potential participation of extrinsic pathways in neuronal cell death after SAH.

Even though our data showed that tozasertib decreased DLK and reduced TUNEL positive neuronal cells. But we cannot rule out that tozasertib may reduce neuronal apoptosis by other signal pathways entirely different from DLK/JIP3/MA2K7/JNK pathway. Since DLK/JIP3/MA2K7 siRNA knocked down DLK, JIP3 and MA2K7 expression and countered the positive effect of tozasertib on neurobehavioral deficits, brain edema and CC-3, it is likely that DLK/JIP3/MA2K7 participated in the anti-apoptotic effect of tozasertib. It has been suggested that DLK is a member of MA3K family and MA2K7 belongs to MA2K family, and both activate the subsequent downstream JNK (a member of MAK family) (Tedeschi and Bradke, 2013). Therefore, we tested JNK and its associated pathways. Interestingly, the JNK inhibitor SP600125 and p38MAPK inhibitor SB203580 markedly countered the inhibitory action of tozasertib on neurobehavioral deficits, brain edema and CC-3. In addition, even though our data demonstrated that tozasertib is effective in the reduction of apoptosis and improved neurological functions, these observations were made in a rat model of SAH, and the potential toxicity has not been clarified, even though we did not observed any apparent toxicity after tozasertib treatment. The molecular weight of tozasertib is 464 which may not be to pass the blood-brain barrier. In this study we used intracerebroventricular injection and other translatable means of administering tozasertib need to be developed and tested.

Overall, tozasertib is effective to reduce neuronal death, decrease brain edema, and improve neurological function, and has potentials to attenuate early brain injury after SAH. The neuroprotective effect of tozasertib may be mediated by DLK/JIP3/MA2K7/JNK pathways and these observations may provide new avenues for treatment of SAH patients.

Acknowledgments

References

Bai JA, Xu GF, Yan LJ, Zeng WW, Ji QQ, Wu JD, Tang QY. SGK1 inhibits cellular apoptosis and promotes proliferation via the MEK/ERK/p53 pathway in colitis. World J Gastroenterol. 2015; 21:6180–6193. [PubMed: 26034353]

Bloom AJ, Miller BR, Sanes JR, DiAntonio A. The requirement for Phr1 in CNS axon tract formation reveals the corticostriatal boundary as a choice point for cortical axons. Genes Dev. 2007; 21:2593–2606. [PubMed: 17901218]

Cahill J, Calvert JW, Zhang JH. Mechanisms of early brain injury after subarachnoid hemorrhage. J Cereb Blood Flow Metab. 2006; 26:1341–1353. [PubMed: 16482081]

Caner B, Hou J, Altay O, Fujii M, Zhang JH. Transition of research focus from vasospasm to early brain injury after subarachnoid hemorrhage. J Neurochem. 2012; 123(Suppl 2):12–21. [PubMed: 23050638]

Chang F, Steelman LS, Shelton JG, Lee JT, Navolanic PM, Blalock WL, Franklin R, McCubrey JA. Regulation of cell cycle progression and apoptosis by the Ras/Raf/MEK/ERK pathway (Review). Int J Oncol. 2003; 22:469–480. [PubMed: 12579299]

Chen Q, Zhang J, Guo J, Tang J, Tao Y, Li L, Feng H, Chen Z. Chronic hydrocephalus and perihematomal tissue injury developed in a rat model of intracerebral hemorrhage with ventricular extension. Transl Stroke Res. 2015; 6:125–132. [PubMed: 25167916]

Chen S, Feng H, Sherchan P, Klebe D, Zhao G, Sun X, Zhang J, Tang J, Zhang JH. Controversies and evolving new mechanisms in subarachnoid hemorrhage. Prog Neurobiol. 2013a; 115:64–91. [PubMed: 24076160]

Chen S, Ma Q, Krafft PR, Chen Y, Tang J, Zhang J, Zhang JH. P2X7 receptor antagonism inhibits p38 mitogen-activated protein kinase activation and ameliorates neuronal apoptosis after subarachnoid hemorrhage in rats. Crit Care Med. 2013b; 41:e466–474. [PubMed: 23963136]

Chen X, Rzhetskaya M, Kareva T, Bland R, During MJ, Tank AW, Kholodilov N, Burke RE. Antiapoptotic and trophic effects of dominant-negative forms of dual leucine zipper kinase in dopamine neurons of the substantia nigra in vivo. J Neurosci. 2008; 28:672–680. [PubMed: 18199767]

Etminan N. Aneurysmal subarachnoid hemorrhage--status quo and perspective. Transl Stroke Res. 2015; 6:167–170. [PubMed: 25860440]

Feng ZP, Deng HC, Jiang R, Du J, Cheng DY. Involvement of AP-1 in p38MAPK signaling pathway in osteoblast apoptosis induced by high glucose. Genet Mol Res. 2015; 14:3149–3159. [PubMed: 25966080]

Ferraris D, Yang Z, Welsbie D. Dual leucine zipper kinase as a therapeutic target for neurodegenerative conditions. Future Med Chem. 2013; 5:1923–1934. [PubMed: 24175744]

Garcia JH, Wagner S, Liu KF, Hu XJ. Neurological deficit and extent of neuronal necrosis attributable to middle cerebral artery occlusion in rats. Statistical validation. Stroke. 1995; 26:627–634. discussion 635. [PubMed: 7709410]

Ghosh AS, Wang B, Pozniak CD, Chen M, Watts RJ, Lewcock JW. DLK induces developmental neuronal degeneration via selective regulation of proapoptotic JNK activity. J Cell Biol. 2011; 194:751–764. [PubMed: 21893599]

Grunwald IQ, Kuhn AL, Schmitt AJ, Balami JS. Aneurysmal SAH: current management and complications associated with treatment and disease. J Invasive Cardiol. 2014; 26:30–37. [PubMed: 24402809]

Harrington EA, Bebbington D, Moore J, Rasmussen RK, Ajose-Adeogun AO, Nakayama T, Graham JA, Demur C, Hercend T, Diu-Hercend A, Su M, Golec JM, Miller KM. VX-680, a potent and selective small-molecule inhibitor of the Aurora kinases, suppresses tumor growth in vivo. Nat Med. 2004; 10:262–267. [PubMed: 14981513]

Hasegawa Y, Suzuki H, Uekawa K, Kawano T, Kim-Mitsuyama S. Characteristics of Cerebrovascular Injury in the Hyperacute Phase After Induced Severe Subarachnoid Hemorrhage. Transl Stroke Res. 2015; 6:458–466. [PubMed: 26358229]

Hirai S, Banba Y, Satake T, Ohno S. Axon formation in neocortical neurons depends on stage-specific regulation of microtubule stability by the dual leucine zipper kinase-c-Jun N-terminal kinase pathway. J Neurosci. 2011; 31:6468–6480. [PubMed: 21525288]

Hirai S, Cui de F, Miyata T, Ogawa M, Kiyonari H, Suda Y, Aizawa S, Banba Y, Ohno S. The c-Jun N-terminal kinase activator dual leucine zipper kinase regulates axon growth and neuronal migration in the developing cerebral cortex. J Neurosci. 2006; 26:11992–12002. [PubMed: 17108173]

Hirai S, Kawaguchi A, Hirasawa R, Baba M, Ohnishi T, Ohno S. MAPK-upstream protein kinase (MUK) regulates the radial migration of immature neurons in telencephalon of mouse embryo. Development. 2002; 129:4483–4495. [PubMed: 12223406]

Huang XF, Luo SK, Xu J, Li J, Xu DR, Wang LH, Yan M, Wang XR, Wan XB, Zheng FM, Zeng YX, Liu Q. Aurora kinase inhibitory VX-680 increases Bax/Bcl-2 ratio and induces apoptosis in Aurora-A-high acute myeloid leukemia. Blood. 2008; 111:2854–2865. [PubMed: 18160664]

Itoh A, Horiuchi M, Wakayama K, Xu J, Bannerman P, Pleasure D, Itoh T. ZPK/DLK, a mitogen-activated protein kinase kinase kinase, is a critical mediator of programmed cell death of motoneurons. J Neurosci. 2011; 31:7223–7228. [PubMed: 21593306]

Krantic S, Mechawar N, Reix S, Quirion R. Apoptosis-inducing factor: a matter of neuron life and death. Prog Neurobiol. 2007; 81:179–196. [PubMed: 17267093]

Kusaka G, Ishikawa M, Nanda A, Granger DN, Zhang JH. Signaling pathways for early brain injury after subarachnoid hemorrhage. J Cereb Blood Flow Metab. 2004; 24:916–925. [PubMed: 15362722]

Li H, Gao A, Feng D, Wang Y, Zhang L, Cui Y, Li B, Wang Z, Chen G. Evaluation of the protective potential of brain microvascular endothelial cell autophagy on blood-brain barrier integrity during experimental cerebral ischemia-reperfusion injury. Transl Stroke Res. 2014; 5:618–626. [PubMed: 25070048]

Liu F, Hu Q, Li B, Manaenko A, Chen Y, Tang J, Guo Z, Tang J, Zhang JH. Recombinant Milk Fat Globule-EGF Factor-8 Reduces Oxidative Stress via Integrin beta3/Nuclear Factor Erythroid 2-Related Factor 2/Heme Oxygenase Pathway in Subarachnoid Hemorrhage Rats. Stroke. 2014

Mata M, Merritt SE, Fan G, Yu GG, Holzman LB. Characterization of dual leucine zipper-bearing kinase, a mixed lineage kinase present in synaptic terminals whose phosphorylation state is regulated by membrane depolarization via calcineurin. J Biol Chem. 1996; 271:16888–16896. [PubMed: 8663324]

Merritt SE, Mata M, Nihalani D, Zhu C, Hu X, Holzman LB. The mixed lineage kinase DLK utilizes MKK7 and not MKK4 as substrate. J Biol Chem. 1999; 274:10195–10202. [PubMed: 10187804]

Michaelis M, Selt F, Rothweiler F, Loschmann N, Nusse B, Dirks WG, Zehner R, Cinatl J Jr. Aurora kinases as targets in drug-resistant neuroblastoma cells. PLoS One. 2014; 9:e108758. [PubMed: 25268132]

Song J, Li P, Chaudhary N, Gemmete JJ, Thompson BG, Xi G, Pandey AS. Correlating Cerebral (18)FDG PET-CT Patterns with Histological Analysis During Early Brain Injury in a Rat Subarachnoid Hemorrhage Model. Transl Stroke Res. 2015; 6:290–295. [PubMed: 25833084]

Sugawara T, Ayer R, Jadhav V, Zhang JH. A new grading system evaluating bleeding scale in filament perforation subarachnoid hemorrhage rat model. J Neurosci Methods. 2008; 167:327–334. [PubMed: 17870179]

Suwatcharangkoon S, Meyers E, Falo C, Schmidt JM, Agarwal S, Claassen J, Mayer SA. Loss of Consciousness at Onset of Subarachnoid Hemorrhage as an Important Marker of Early Brain Injury. JAMA Neurol. 2015:1–8. [PubMed: 26659895]

Tang J, Hu Q, Chen Y, Liu F, Zheng Y, Zhang J, Zhang JH. Neuroprotective Role of an N-acetyl Serotonin Derivative via Activation of Tropomyosin-related Kinase Receptor B after Subarachnoid Hemorrhage in a Rat Model. Neurobiol Dis. 2015

Tedeschi A, Bradke F. The DLK signalling pathway--a double-edged sword in neural development and regeneration. EMBO Rep. 2013; 14:605–614. [PubMed: 23681442]

Topkoru BC, Altay O, Duris K, Krafft PR, Yan J, Zhang JH. Nasal administration of recombinant osteopontin attenuates early brain injury after subarachnoid hemorrhage. Stroke. 2013; 44:3189–3194. [PubMed: 24008574]

Tu XK, Yang WZ, Chen JP, Chen Y, Chen Q, Chen PP, Shi SS. Repetitive ischemic preconditioning attenuates inflammatory reaction and brain damage after focal cerebral ischemia in rats: involvement of PI3K/Akt and ERK1/2 signaling pathway. J Mol Neurosci. 2015; 55:912–922. [PubMed: 25338292]

Tyler RK, Shpiro N, Marquez R, Eyers PA. VX-680 inhibits Aurora A and Aurora B kinase activity in human cells. Cell Cycle. 2007; 6:2846–2854. [PubMed: 18032922]

Watkins TA, Wang B, Huntwork-Rodriguez S, Yang J, Jiang Z, Eastham-Anderson J, Modrusan Z, Kaminker JS, Tessier-Lavigne M, Lewcock JW. DLK initiates a transcriptional program that couples apoptotic and regenerative responses to axonal injury. Proc Natl Acad Sci U S A. 2013; 110:4039–4044. [PubMed: 23431164]

Wei X, Ren X, Jiang R, Li H, Gao F, Chen Y, Hou J, Liu X, Sun S, Yang M. Phosphorylation of p38 MAPK mediates aquaporin 9 expression in rat brains during permanent focal cerebral ischaemia. J Mol Histol. 2015; 46:273–281. [PubMed: 25903824]

Welsbie DS, Yang Z, Ge Y, Mitchell KL, Zhou X, Martin SE, Berlinicke CA, Hackler L Jr, Fuller J, Fu J, Cao LH, Han B, Auld D, Xue T, Hirai S, Germain L, Simard-Bisson C, Blouin R, Nguyen JV, Davis CH, Enke RA, Boye SL, Merbs SL, Marsh-Armstrong N, Hauswirth WW, DiAntonio A, Nickells RW, Inglese J, Hanes J, Yau KW, Quigley HA, Zack DJ. Functional genomic screening identifies dual leucine zipper kinase as a key mediator of retinal ganglion cell death. Proc Natl Acad Sci U S A. 2013; 110:4045–4050. [PubMed: 23431148]

Yatsushige H, Yamaguchi-Okada M, Zhou C, Calvert JW, Cahill J, Colohan AR, Zhang JH. Inhibition of c-Jun N-terminal kinase pathway attenuates cerebral vasospasm after experimental subarachnoid hemorrhage through the suppression of apoptosis. Acta Neurochir Suppl. 2008; 104:27–31. [PubMed: 18456994]

Zhan Y, Krafft PR, Lekic T, Ma Q, Souvenir R, Zhang JH, Tang J. Imatinib preserves blood-brain barrier integrity following experimental subarachnoid hemorrhage in rats. J Neurosci Res. 2015; 93:94–103. [PubMed: 25196554]

Highlights

Subarachnoid hemorrhage caused brain edema and blood-brain barrier rupture in a rat model.

Tozasertib reduced these brain injuries and improved neurological function.

The mechanisms of Tozasertib may be mediated by dual leucine zipper kinase (DLK) which belongs to mitogen-activated protein kinase kinase family.

The downstream signaling for Tozasertib in subarachnoid hemorrhage may be related to JIP3, MA2K7, JNK and Caspase-3.

Tozasertib is a molecular-targeted compound and used in clinical trials for keukimia and therefore is translatable.
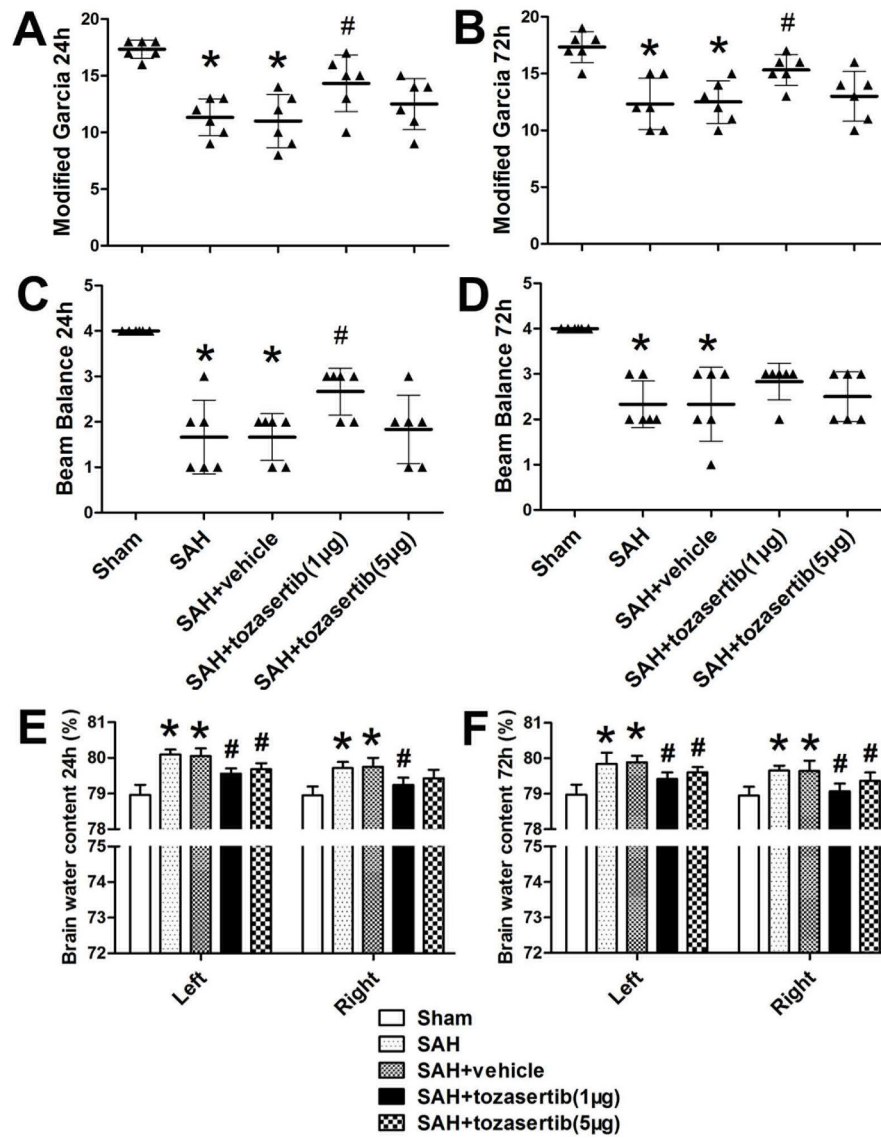
Fig. 1.

The effect of tozasertib on the neurobehavioral function and brain edema at 24 and 72 hours after SAH. At 24 hours after SAH: **A**, when compare with Sham group, SAH reduced modified Garcia score and tozasertib at lower (1μg) but not higher (5μg) concentration improved neurological function. **C**, When compare with Sham, SAH reduced beam balance score and tozasertib at lower (1μg) but not higher (5μg) concentration improved beam balance score. **E,** SAH increased brain water content and tozasertib at both low (1μg) and high (5μg) concentrations reduced brain water content, but tozasertib (5μg) failed to significantly reduced brain water content in right hemisphere.

At 72 hours after SAH: **B**, When compare with Sham group, SAH reduced modified Garcia score and tozasertib at lower (1μg) but not higher (5μg) concentrations improved neurological function. **D**, When compare with Sham, SAH reduced beam balance score and tozasertib at lower (1μg) and higher (5μg) concentrations failed to improve beam balance

score. **F,** SAH increased brain water content and tozasertib at both low (1μg) and high (5μg) concentrations reduced brain water content. *p<0.05 vs sham, #p<0.05 vs SAH/SAH +vehicle.
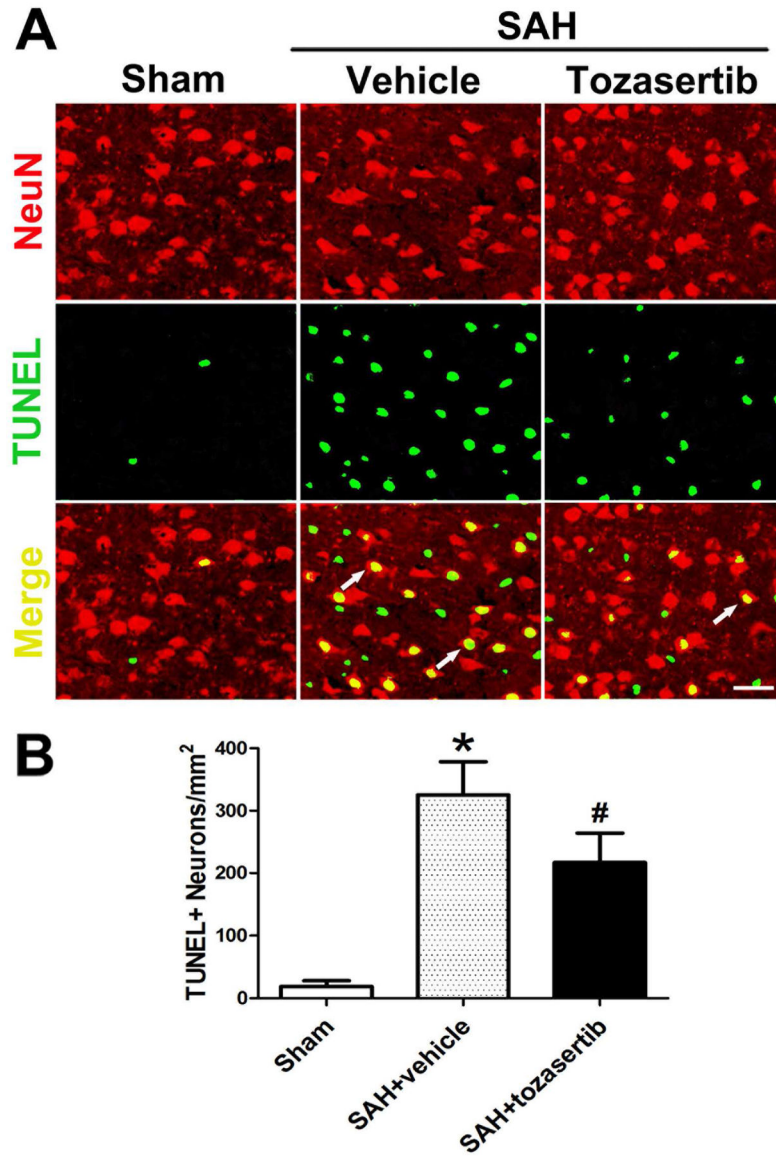
Fig. 2.

Tozasertib reduced TUNEL positive neurons at 24 hours after SAH. **A**. Representative immunofluorescence staining showed TUNEL and NeuN double-stained cells (TUNEL +neurons) of the left cortex in sham, SAH+vehicle, and SAH+tozasertib (1μg) groups. **B**. More TUNEL positive neurons are observed in vehicle treated animals and tozasertib (1μg) decreased the number of TUNEL-positive cells. Scale bar, 30 μm. $*p<0.05$ vs sham, $\#p<0.05$ vs SAH+vehicle.
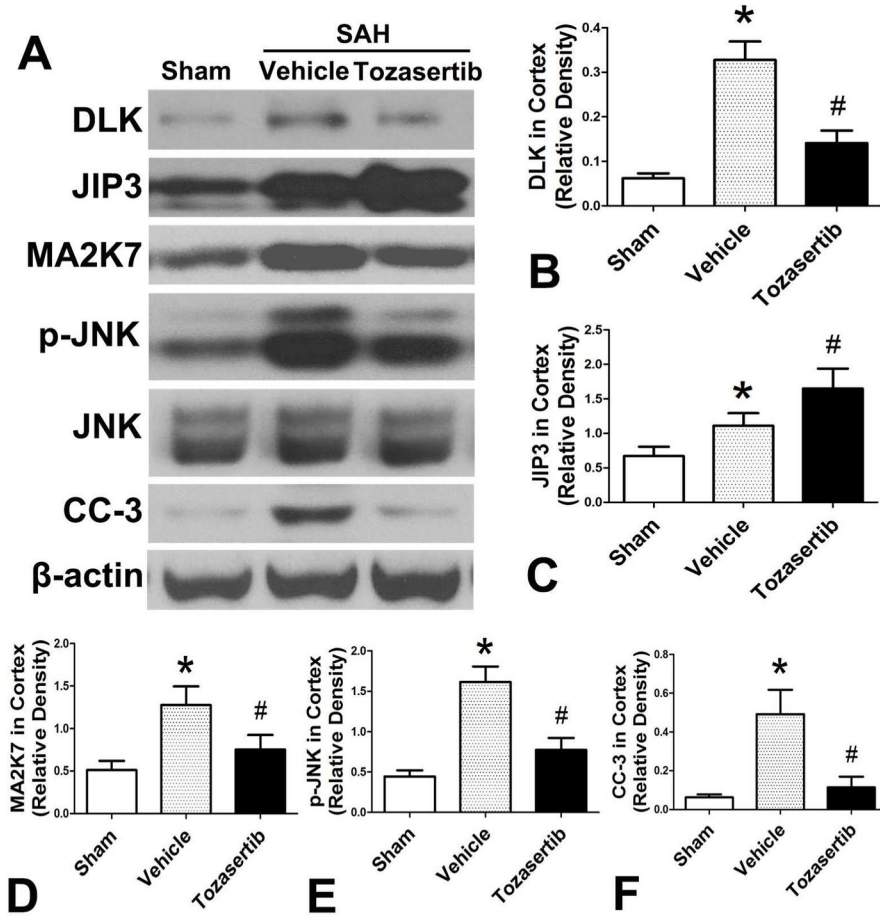
Fig. 3.
Effects of tozasertib on the expression of DLK/JIP3/MA2K7/p-JNK/CC-3 in the left cortex at 24 hours after SAH. **A**, Representative western blots. **B, C, D, E, F,** Quantitative analysis of DLK, JIP3, MA2K7, p-JNK, and CC-3. *$p<0.05$ vs sham, #$p<0.05$ vs SAH+vehicle.
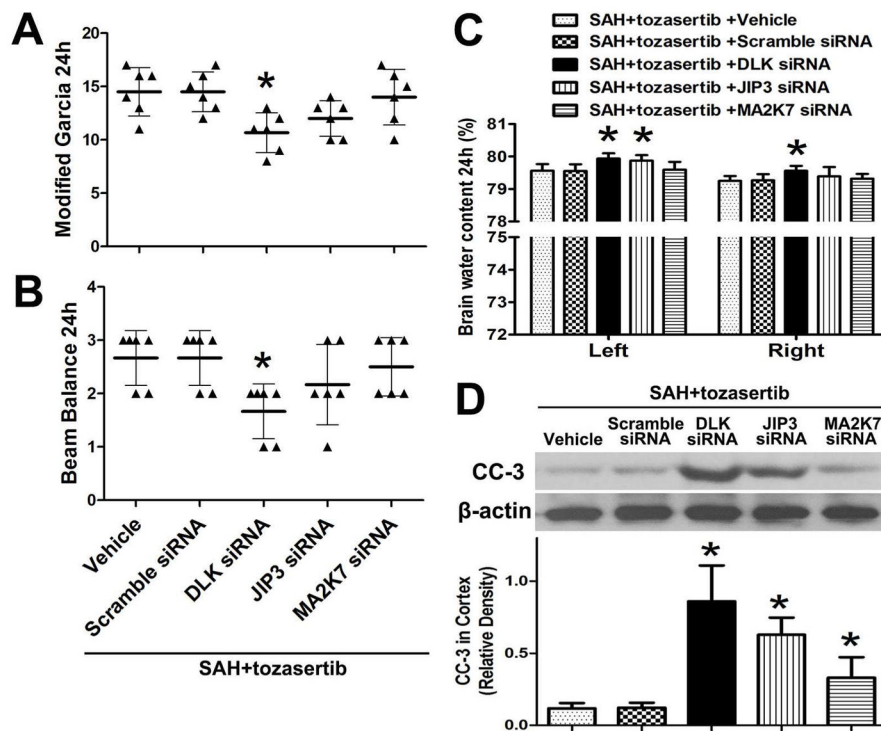
Fig. 4.
Effects of DLK/JIP3/MA2K7 siRNA on the inhibitory action of tozasertib on neurobehavioral deficits, brain edema and CC-3 at 24 hours after SAH. **A, B,** DLK siRNA significantly attenuated the positive effects of tozasertib on modified Garcia and beam balance score. The JIP3/MA2K7 siRNA did not significantly attenuate above effects. **C,** DLK siRNA countered the positive effects of tozasertib on brain edema in left and right hemispheres of the brain. JIP3 siRNA only countered the above mentioned effect of tozasertib in left hemispheres of the brain. The MA2K7 siRNA did not significantly attenuate above mentioned effects. **D,** DLK, JIP3 and MA2K7 siRNA countered the inhibitory effect of tozasertib on CC-3 expression in the left cortex. **Top,** Representative western blots. **Bottom,** Quantitative analysis of CC-3. *$p < 0.05$ vs SAH+tozasertib +vehicle/SAH+tozasertib+scramble siRNA.
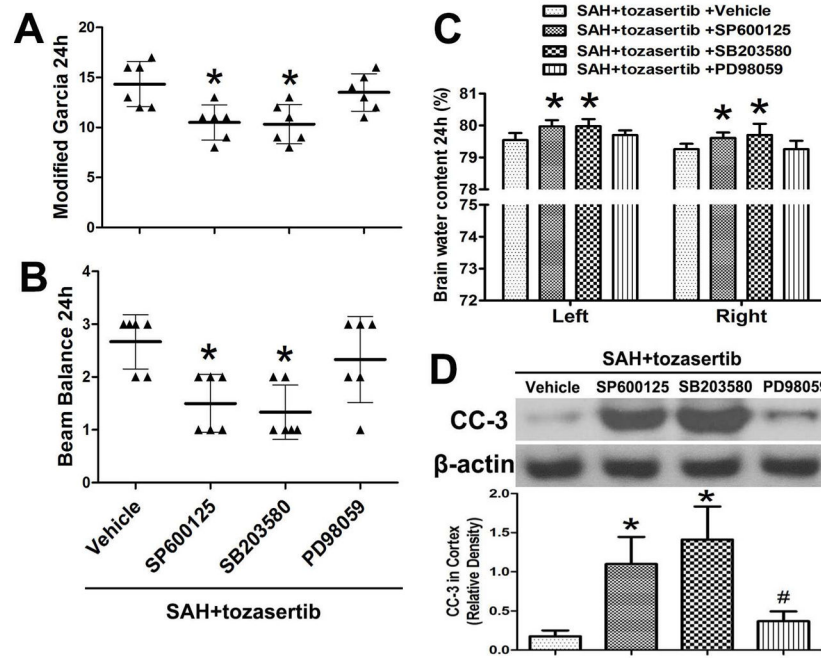
Fig. 5.
Effects of JNK/p38MAPK/MEK inhibitors SP600125, SB203580, and PD98059, respectively, on the inhibitory action of tozasertib on neurobehavioral deficits, brain edema and CC-3 at 24 hours after SAH. **A, B,** JNK/p38MAPK inhibitors significantly inhibited the positive effects of tozasertib on modified Garcia and beam balance score. The MEK inhibitor did not significantly inhibit above mentioned effects. **C,** JNK/p38MAPK inhibitors obviously inhibited the positive effects of tozasertib on brain edema in left and right hemispheres of the brain. The MEK inhibitor did not obviously inhibit above mentioned effects. **D,** In the presence of tozasertib and after SAH, CC-3 level was reduced by tozasertib. JNK/p38MAPK/MEK inhibitors countered the inhibitory effect of tozasertib on CC-3 expression in the left cortex. **Top,** Representative western blots. **Bottom,** Quantitative analysis of CC-3. *$p < 0.05$ vs SAH+tozasertib+vehicle, #$p > 0.05$ vs SAH+tozasertib +SP600125/SAH+tozasertib+SB203580.
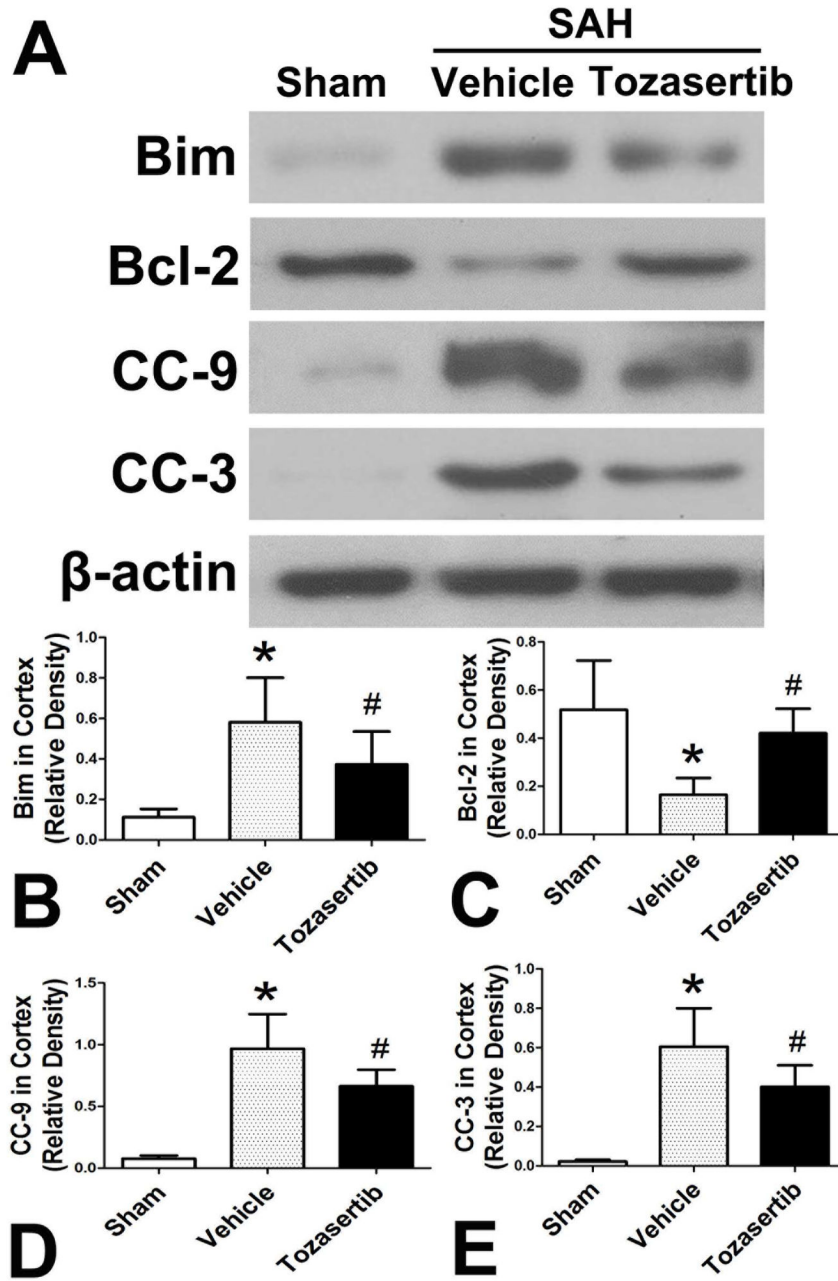
Fig. 6.
Effect of tozasertib on other apoptosis factors in the left cortex at 24 hours after SAH. **A,** Representative western blots. **B, C, D, E,** Quantitative analysis of Bim, Bcl-2, CC-9, CC-3. *$p < 0.05$ vs sham, #$p < 0.05$ vs SAH+vehicle.